JACS
JOURNAL OF THE AMERICAN CHEMICAL SOCIETY

Article

pubs.acs.org/JACS

Two-Fold Odd–Even Effect in Self-Assembled Nanowires from Oligopeptide-Polymer-Substituted Perylene Bisimides

Roman Marty, Robin Nigon, Deborah Leite, and Holger Frauenrath*

Ecole Polytechnique Fédérale de Lausanne (EPFL), Institute of Materials, Laboratory of Macromolecular and Organic Materials, EPFL – STI – IMX – LMOM, MXG 037, Station 12 1015 Lausanne, Switzerland

Supporting Information

ABSTRACT: Organic nanowires are important building blocks for nanoscopic organic electronic devices. In order to ensure efficient charge transport through such nanowires, it is important to understand in detail the molecular parameters that guide self-assembly of π-conjugated molecules into one-dimensional stacks with optimal constructive $\pi-\pi$ overlap. Here, we investigated the subtle relationship between molecular structure and supramolecular arrangement of the chromophores in self-assembled nanowires prepared from perylene bisimides with oligopeptide-polymer side chains. We observed a "two-fold" odd–even effect in circular dichroism spectra of these derivatives, depending on both the number of L-alanine units in the oligopeptide segments and length of the alkylene spacer between chromophore and oligopeptide substituents. Our results indicate that there is a complex interplay between the translation of molecular chirality into supramolecular helicity and the molecules' inherent propensity for well-defined one-dimensional aggregation into β-sheet-like superstructures in the presence of a central chromophore. Strong excitonic coupling as expressed by the appearance of hypsochromically and bathochromically shifted UV–vis absorptions and strong CD signals was systematically observed for molecules with an odd number of L-alanines in the side chains. The latter derivatives gave rise to nanowires with a significantly higher electron mobility. Our results, hence, provide an important design rule for self-assembled organic nanowires.

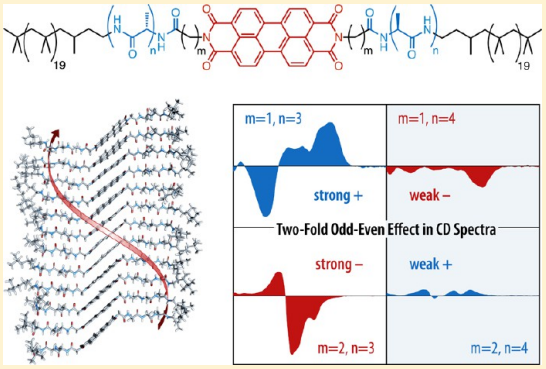

INTRODUCTION

One-dimensional nanowires from π-conjugated polymers and small molecules[1,2] are important building blocks for the fabrication of nanoelectronic devices such as organic field-effect transistors and nanoelectric ciruits,[3−9] solar cells,[10−14] or chemical sensors.[15−19] The capability to efficiently transport charge carriers through such nanowires ultimately depends on the nature of the charge percolation paths which result from a delicate balance between $\pi-\pi$ and other supramolecular interactions. In this regard, bottom-up self-assembly offers the unique opportunity to obtain organic nanowires of which the morphology is strictly controlled by the underlying molecular design. Chromophores bearing chiral substituents[20−22] including short oligopeptides,[23] for example, have frequently been employed to induce the formation of helical supramolecular assemblies. However, a better understanding of which molecular parameters positively affect the π-overlap between adjacent chromophores is still needed in order to obtain supramolecular systems with improved charge transport properties. Systems that follow simple and general design rules are preferred for this purpose. In this regard, supramolecular helical systems are promising because the relationship between the position and absolute configuration of the stereocenter and helicity has long since been described by the surprisingly universal SED/SOL-rules,[24] that equally apply to most examples of chiral liquid crystal phases,[25,26] helical polymers,[27−29] or self-assembled aggregates.[30]

We recently prepared well-defined supramolecular nanowires from chiral oligopeptide-polymer-substituted quaterthiophenes and perylene bisimides that showed tight $\pi-\pi$ stacking synergistically enhanced by hydrogen bonding between the oligopeptide side groups.[31] Here, we present a comprehensive investigation on the relationship between molecular structure and internal arrangement of the chromophores within self-assembled perylene bisimide nanowires. Our results show that, in these systems, there is a complex interplay between the universal translation of molecular chirality into supramolecular helicity and the molecules' inherent propensity to form β-sheet-like one-dimensional aggregates, encoded by the oligopeptide segments. The result is the first example of a "two-fold" odd–even effect in circular dichroism (CD) spectra, depending on both the number of L-alanine units in the oligopeptides and length of the alkylene spacer between chromophores and oligopeptide substituent. We, hence, demonstrate that subtle modifications in the molecular structure will strongly influence the exact molecular arrangement of the π-conjugated chromophores in the otherwise well-understood formation of

Received: December 5, 2013
Published: February 14, 2014

   dx.doi.org/10.1021/ja412384p | J. Am. Chem. Soc. 2014, 136, 3919–3927

Scheme 1. Perylene Bisimides 1a−4a, 1b−4b, 2c, and 3c Investigated in this Study[a]

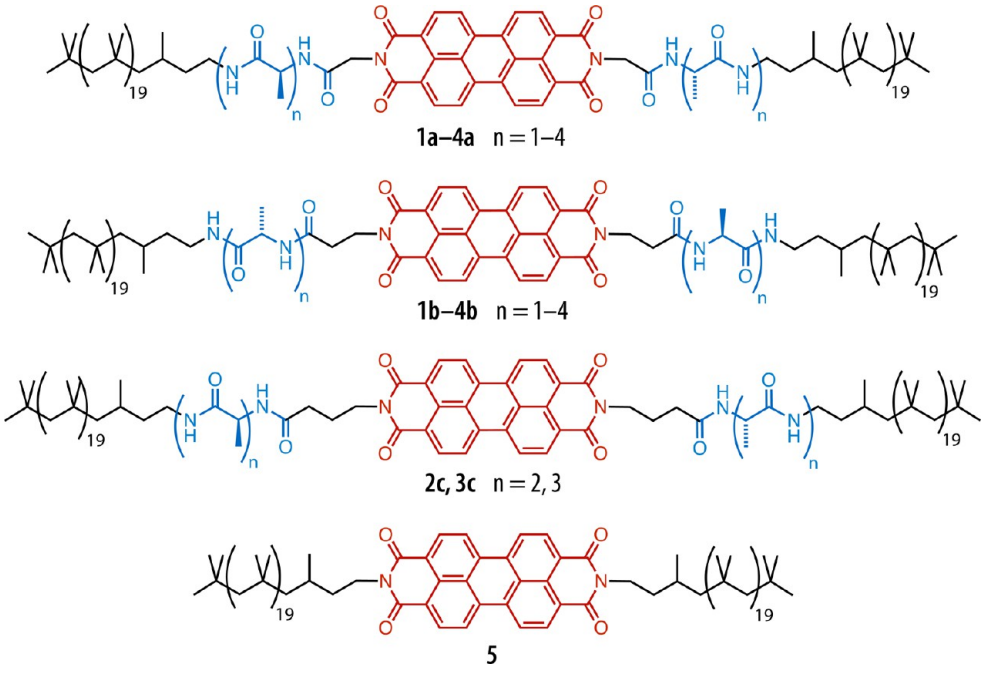

[a]Perylene bisimides **1a−4a**, **1b−4b**, **2c**, and **3c** bear oligopeptide-polymer substituents that comprise n = 1−4 L-alanine units (blue) separated from the chromophore (red) by a flexible methylene, ethylene, or propylene spacer. The polymer-functionalized perylene bisimide **5** served as a nonaggregating reference compound.

nanowires from oligopeptide-polymer-substituted π-conjugated molecules. Moreover, we found that charge carrier mobility in field-effect transistors fabricated from nanowire films was correlated with the observed CD intensity that results from excitonic coupling and may be regarded as a proxy for constructive π-overlap between the close packed chromophores. Our findings, thus, demonstrate that the mere formation of one-dimensional aggregates is not a sufficient prerequisite for charge transport, and they provide important design rules for self-assembled organic nanowires.

RESULTS AND DISCUSSION

Synthesis and Aggregation in Solution. For our investigations, we prepared a library of the oligopeptide-polymer-functionalized perylene bisimides **1a−4a**, **1b−4b**, **2c**, and **3c** with a variable number of n = 1−4 L-alanine units (corresponding to the compound numbers **1−4**) as well as methylene, ethylene, and propylene spacers (represented by the labels **a−c** in the compound numbers) between chromophores and oligopeptides (Scheme 1). The polymer-functionalized perylene bisimide **5** served as a nonaggregating reference compound. All compounds were synthesized by simple solution-phase peptide coupling and deprotection reactions starting from poly(isobutylene) amine and appropriate perylene bisimide building blocks (Schemes S1−S5), similar to previously published strategies.[32,33]

Optically clear dispersions of **1a−4a**, **1b−4b**, **2c**, and **3c** were obtained upon thorough thermal annealing in 1,1,2,2-tetrachloroethane (TCE), which provides a hydrophobic environment to induce strong hydrogen-bonding of the oligopeptides but is a good solvent for the attached poly(isobutylene) segments.[31]

The combination of solution-phase infrared (IR), UV−vis, and CD spectroscopy as well as atomic force microscopy (AFM) proved that all derivatives gave rise to one-dimensional, hydrogen-bonded aggregates in organic solvents that exhibited $\pi-\pi$ stacked chromophores in a helical arrangement. For instance, the strong absorption bands in the solution-phase IR spectra of all compounds at 3290−3296 cm^{-1} in the amide A region and at 1626−1639 cm^{-1} in the amide I region, as well as the absence of the secondary amide I component at around 1695 cm^{-1} were all consistent with the formation of strongly hydrogen-bonded, parallel β-sheet-like aggregates (Figure 1a). The very weak bands observed at 3408−3431 cm^{-1} in some cases may indicate the presence of miniscule amounts of residual nonaggregated molecules, and the absorptions at around 1700, 1665, and 1595 cm^{-1} represent the C═O and C═C vibrations of the perylene bisimide core.[34] Plotting the relative peak area $A_{3290}/A_{\text{amide A}}$ obtained by peak deconvolution versus the number of L-alanines in each side group revealed that all derivatives were fully aggregated in solution (Figure 1b). This is also reflected in the observed linear increase of $A_{1630}/A_{\text{amide I}}$ with increasing number of L-alanines, as each additional amide carbonyl group linearly contributes to the overall absorption intensity.

In order to confirm the presence of nanowires comprising a single stack of one-dimensionally aggregated perylene bisimides, atomic force microscopy (AFM) images of **1a−4a**, **1b−4b**, **2c**, and **3c** on mica substrates were recorded at concentrations 100 times lower than those used in IR spectroscopy (Figure 2a). For this reason, the effect of dilution onto aggregate stability was investigated by comparing the UV−vis spectra obtained from a concentration series (Figure S1). While **1b** was found to deaggregate to some degree, and minor differences were also observed in the UV−vis spectra of **1a**, **2b**, and **2c** upon dilution from 1×10^{-3} to 1×10^{-5} mol/L, the UV−vis spectra of all other compounds remained unaffected. Indeed, AFM imaging proved that all molecules

dx.doi.org/10.1021/ja412384p | J. Am. Chem. Soc. 2014, 136, 3919−3927

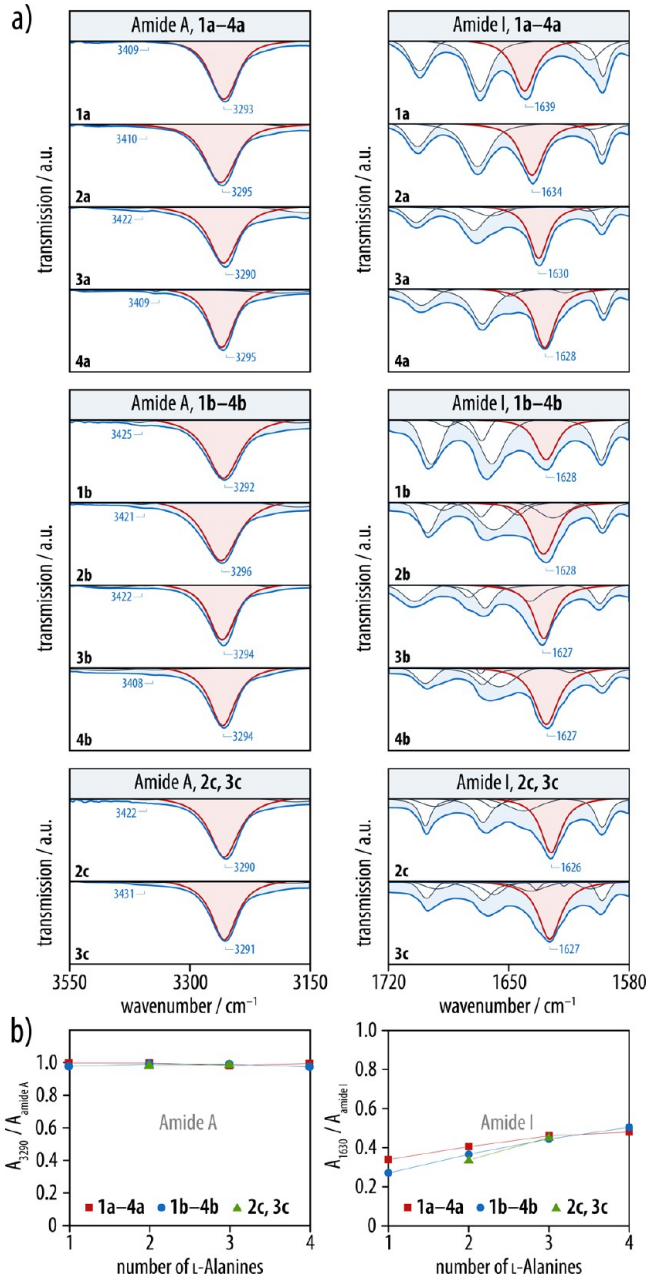

Figure 1. (a) The amide A and amide I regions of the solution-phase IR spectra ($c = 1 \times 10^{-3}$ mol/L, TCE) of **1a–4a**, **1b–4b**, **2c**, and **3c** exhibited strong absorption bands at around 3290 cm^{-1} and 1630 cm^{-1} (red) that are characteristic for oligopeptides strongly aggregated into parallel β-sheet-like secondary structures. The remaining strong absorptions in the amide I region (blue) are assigned to the perylene bisimide core. (b) A plot of the relative peak area $A_{3290}/A_{amide\ A}$ obtained by peak deconvolution versus the number of L-alanines indicated complete aggregation for all derivatives in solution. This is consistent with the observed quasi-linear increase of $A_{1630}/A_{amide\ I}$ with increasing number of L-alanines because the oscillator strength of each additional amide carboyl group linearly contributes to the overall absorption intensity.

formed well-defined and several micrometers long nanowires. In agreement with the UV–vis measurements, considerable amounts of nonaggregated material were only observed for the less stable aggregates. AFM phase images taken at higher magnification proved that occasionally observed broader features were not larger fibrillar bundles obtained by β-sheet stacking (of the oligopeptide-perylene bisimide cores) but comprised individual nanowires with a defined width of 6–7 nm. As we have shown previously for a related molecule, these dimensions are commensurate with nanowires formed from a single helically arranged stack of molecules.[31]

UV–vis Spectroscopy. Consistent with the results obtained from IR spectroscopy and AFM imaging, the temperature-dependent solution-phase UV–vis spectra of **1a–4a**, **1b–4b**, **2c**, and **3c** at a concentration of 1×10^{-4} mol/L indicated the presence of π–π stacked perylene bisimides at room temperature (Figure 3a, blue). Upon increasing the temperature to 363 K, significant deaggregation was observed for **1b** and **2c**, while **2a** and **2b** partially deaggregated (Figure 3a, red). By contrast, the aggregates of **3a–c**, **4a**, and **4b** bearing $n \geq 3$ L-alanines remained fully aggregated at elevated temperatures, irrespective of spacer length. Qualitative information on the relative aggregate stability was obtained by plotting the normalized difference in extinction at $\lambda = 530$ nm compared to a fully deaggregated compound versus temperature (Figure 3b).[35] These plots clearly demonstrate that, as expected, aggregate stability increased with the number of L-alanine units and that it decreased with spacer length[36] if the number of L-alanines was $n \leq 2$. Moreover, it is interesting to note that a change in spacer length significantly altered the shape of the UV–vis spectra, as well, supposedly as a consequence of subtle differences in the π–π stacking of the perylene bisimides (Figure 3a, bottom right). A blue-shift of the main absorption combined with the simultaneous appearance of bathochromically shifted absorption bands as observed for **3a**, **3b**, **4a**, and **4b** suggested the presence of strongly cofacially aggregated but both laterally and rotationally displaced perylene bisimide cores.[37] By contrast, the mainly red-shifted spectrum of **3c** may be indicative of predominantly laterally and only marginally rotationally displaced arrangement of neighboring perylene bisimide chromophores.

CD Spectroscopy. The influence of subtle changes in the molecular structure on the local arrangement of the chromophores within the aggregates was strongly visible in the CD spectra (Figure 4a). They exhibited different odd–even effects both in terms of shape and intensity of the spectra as well as the signs of the Cotton effects and depended on two molecular parameters at the same time, i.e., the number of L-alanines and the spacer length. A first conspicuous feature observed in the CD series was that, depending on the number of L-alanine units, the observed CD activity was alternatingly strong and weak and, accordingly, the shape of the spectra well- and ill-defined, respectively. Thus, the molecules bearing an odd number of L-alanines in the side chains (**1a**, **1b**, and **3a–c**) exhibited well-defined spectra with molar ellipticities increasing with the number of L-alanine residues (Figure 4, white background). By contrast, the CD spectra of all compounds bearing an even number of L-alanines in the side chains (**2a–c**, **4a**, and **4b**) were considerably less defined and exhibited much smaller molar ellipticities (Figure 4, gray background). As will be discussed in more detail below, possible explanations for this observation include the presence of one-dimensional aggregates with either a small helix pitch, highly dynamic supramolecular helicity, or a mixture of left- and right-handed helical segments. Moreover, we observed a two-fold odd–even effect that was, on one hand, expressed by an alternating reversal of the Cotton effect upon increasing the number of L-alanines within a series of molecules with the same spacer length; on the other hand,

dx.doi.org/10.1021/ja412384p | J. Am. Chem. Soc. 2014, 136, 3919–3927

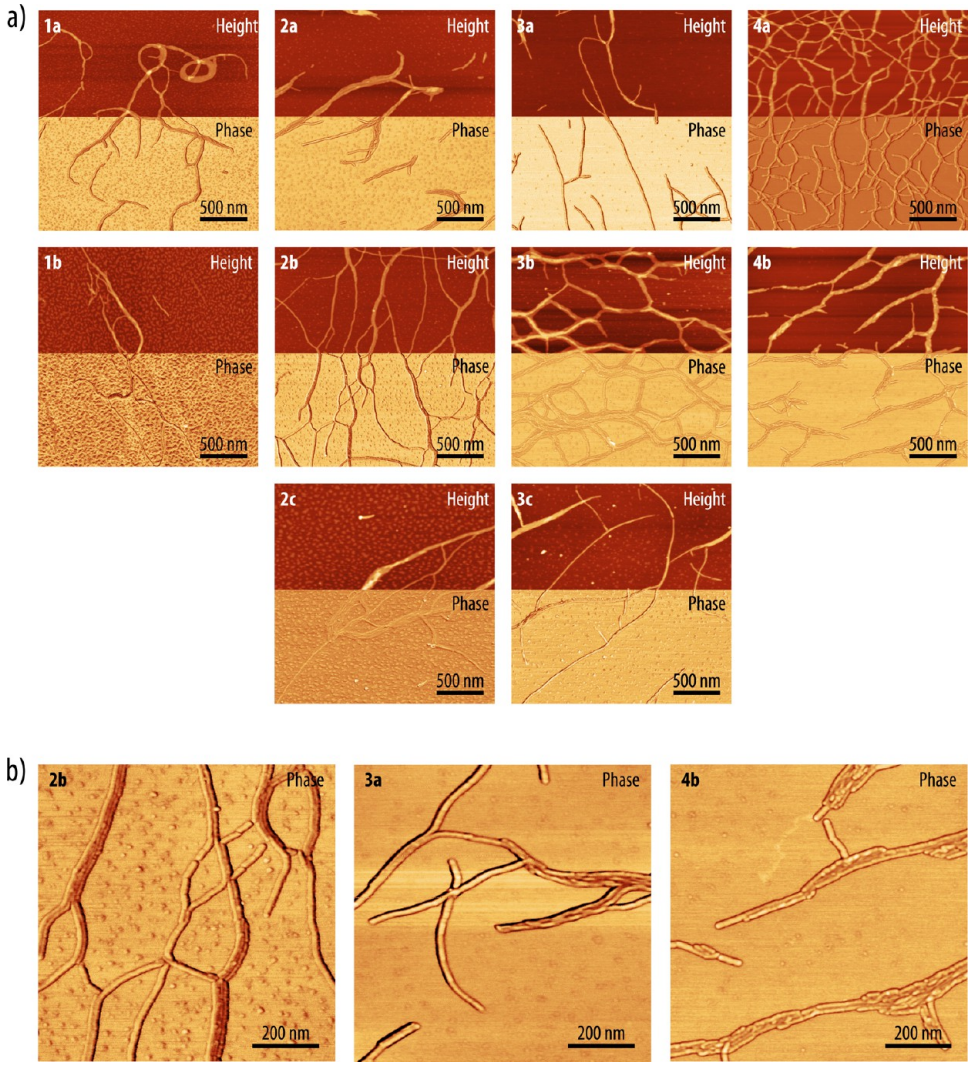

Figure 2. (a) AFM height and phase images of **1a**–**4a**, **1b**–**4b**, **2c**, and **3c** on mica substrates revealed the presence of several micrometers long nanowires; deaggregated material that was formed at the low concentration used to prepare the sample solutions for AFM imaging was only observed for compounds **1a**, **1b**, **2b**, and **2c**. (b) AFM phase images recorded at higher magnification revealed that the occasionally observed broader features were not bundles obtained by β-sheet stacking (of the cores) but consisted of individual nanowires with a width of 6–7 nm, consistent with a single helically arranged stack of molecules.[31]

the sign of the Cotton effect was also alternatingly reversed upon increasing the spacer length for molecules with the identical number of L-alanine units.

We found a positive Cotton effect for **1a**, **2b**, **3a**, **3c**, and **4b** that suggested the presence of *P*-helical (right-handed helical) aggregates (Figure 4, blue); while this assignment is not unambiguous in the case of the only weakly CD-active derivatives **2b** and **4b**, their spectra at least resemble the others in the sign of the key absorption band at 560–570 nm (for the molecules with an ethylene spacer). By contrast, a clearly negative Cotton effect observed for **1b**, **2a**, **2c**, **3b**, and **4a** was assigned to *M*-helical (left-handed helical) aggregates (Figure 4, red).[38,39] These findings appear to partially contradict the empirical SED/SOL-rules, as an *S*-configuration (S) of a stereocenter spaced at an even (E) number of atoms apart from the rigid core would imply an *M*-helical (D) aggregate (note that, in cholesteric liquid crystal phases, the dextro (D) and laevo (L) rotation of linearly polarized light corresponds to left- and right-handed helical molecular arrangements, respectively).[27] According to this nomenclature, derivatives **1a**, **3a**, and **3c** would hence be denoted as SEL, while **1b** and **3b** would be SOD. Different from our derivatives, however, all literature examples obeying the SED/SOL rules possess only one stereocenter per side chain that is connected to the rigid part via either pure alkylene spacers,[25,29] alkylene ethers,[25,27,40] or alkylene esters.[26,28] Notably, no side groups containing hydrogen-bonded amides have been reported, with the exception of asymmetric benzene-1,3,5-tricarboxamides described by Meijer et al.,[41,42] who encountered a similar conflict with the empirical SED/SOL rules. These derivatives formed columnar phases as well as one-dimensional aggregates in dilute solution promoted by intermolecular N–H···O=C-type hydrogen bonding of the amide functionalities, similar to the compounds investigated here. Systems containing at least one amide functionality in the side groups may, hence, inherently behave "anti-SED/SOL".

Structural Interpretation. Attempts to investigate the structural basis for our spectral findings by means of molecular dynamics (MD) simulations at the classical molecular mechanics level showed that, as we had also reported

dx.doi.org/10.1021/ja412384p | J. Am. Chem. Soc. 2014, 136, 3919–3927

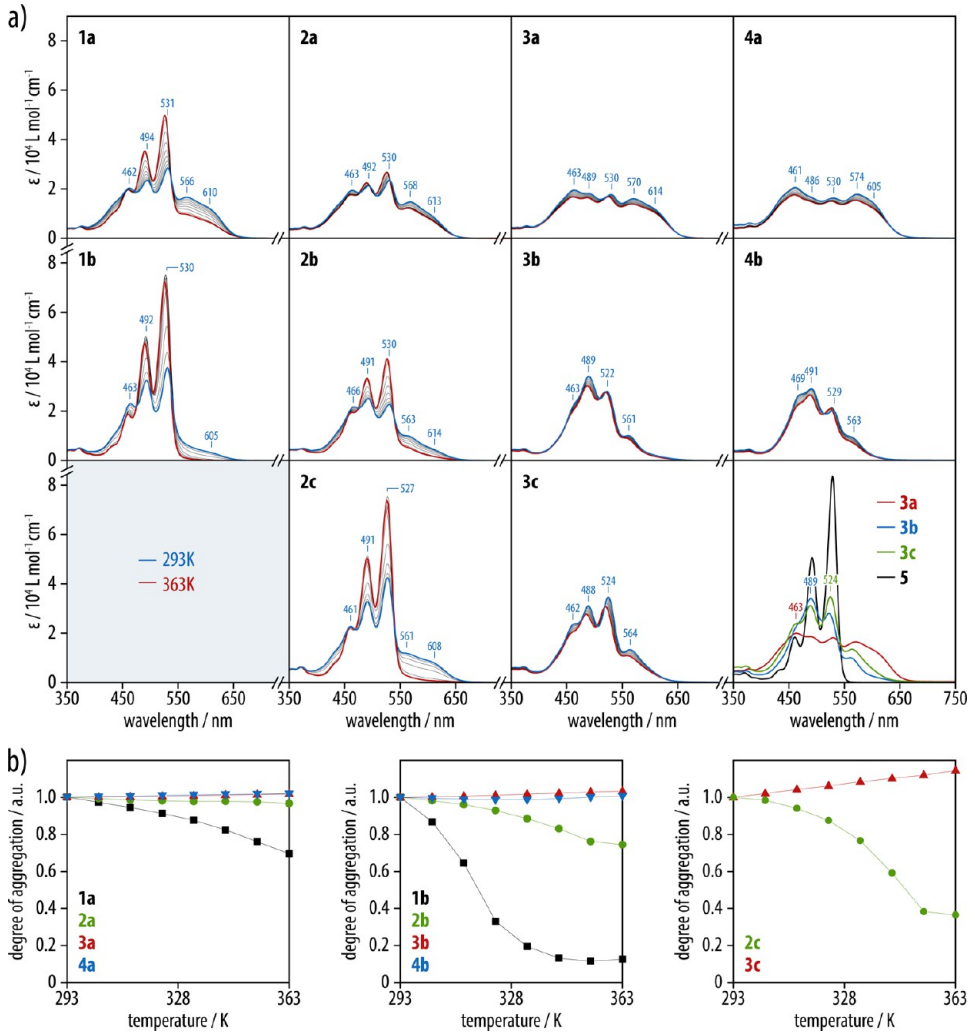

Figure 3. (a) The solution-phase UV−vis spectra at room temperature ($c = 1 \times 10^{-4}$ mol/L, TCE, blue) suggested $\pi-\pi$ stacking of the oligopeptide-polymer-substituted perylene bisimides **1a**−**4a**, **1b**−**4b**, **2c**, and **3c**. By contrast, the UV−vis spectra recorded at 363 K (red) revealed a decreasing stability of the aggregates with increasing spacer length for $n \leq 2$ L-alanine units per side group, while all compounds with $n \geq 3$ L-alanine units were strongly aggregated. The differences observed for **3a**−**c** (bottom right) indicated slightly different geometric arrangements of the chromophores. (b) Qualitative information on aggregate stability was obtained by plotting the degree of aggregation as a function of temperature according to $[\varepsilon(T) - \varepsilon_{mon}]/[\varepsilon_{agg} - \varepsilon_{mon}]$, where ε_{mon} denotes the extinction coefficient (ε) at $\lambda = 530$ nm of the nonaggregated perylene bisimide reference compound **5** at $c = 1 \times 10^{-4}$ mol/L (Figure S2) and $\varepsilon(T)$ and ε_{agg} the ε of the sample at a given temperature T and 293 K, respectively. The slight apparent increase of the degree of aggregation with temperature in some cases may originate from a dilution effect due to thermal expansion of TCE during the experiment.

previously,[31] a determination of both the details of the supramolecular arrangement (the $\pi-\pi$ stacked cores and hydrogen-bonded oligopeptides) and the correct handedness are beyond the accuracy of currently applied state of the art force fields. Nevertheless, our results at least serve to qualitatively illustrate and discuss the experimental observations. Taking dodecameric aggregates of **3a** as a representative example, we were able to construct two different supramolecular arrangements that were both similarly stable and in perfect agreement with X-ray diffraction data. In the first structure (**3a′**), the two innermost oligopeptide carbonyl groups (closest to the chromophore) were oriented in opposite directions parallel to the nanowire axis (Figure 5a). This arrangement leads to an overall zero residual dipole moment from the amide carbonyl groups irrespective of the number of L-alanines and spacer length. However, the placement of the L-alanine methyl groups imposes an unbalanced steric load on the two faces of the aggregates for odd numbers of L-alanines in this case (Figure 5c). In the second model (**3a″**), the two innermost oligopeptide carbonyl groups pointed in the same direction parallel to the nanowire axis (Figure 5b), which results in a balanced placement of the L-alanine methyl groups on the aggregate faces for all derivatives but now induces a nonzero residual dipole moment for an odd number of carbonyl groups, i.e., derivatives with an even number of L-alanines per side chain (Figure 5d).

Interestingly, only **3a′** exhibited a helical arrangement of the chromophores with a defined handedness (albeit the one not coinciding with the experimental results), whereas **3a″** showed a transition from a left- to right-handed arrangement within the same aggregate. If one assumes this ambiguity in the preferred handedness to be the origin of weak CD activity, one must conclude that derivatives with an even number of L-alanines (**2a**−**c**, **4a**−**b**) per side chain follow the second model. The other compounds (**1a**−**b**, **3a**−**c**) would, accordingly, prefer the more intuitive first model, in which the helical arrangement is

dx.doi.org/10.1021/ja412384p | J. Am. Chem. Soc. 2014, 136, 3919−3927

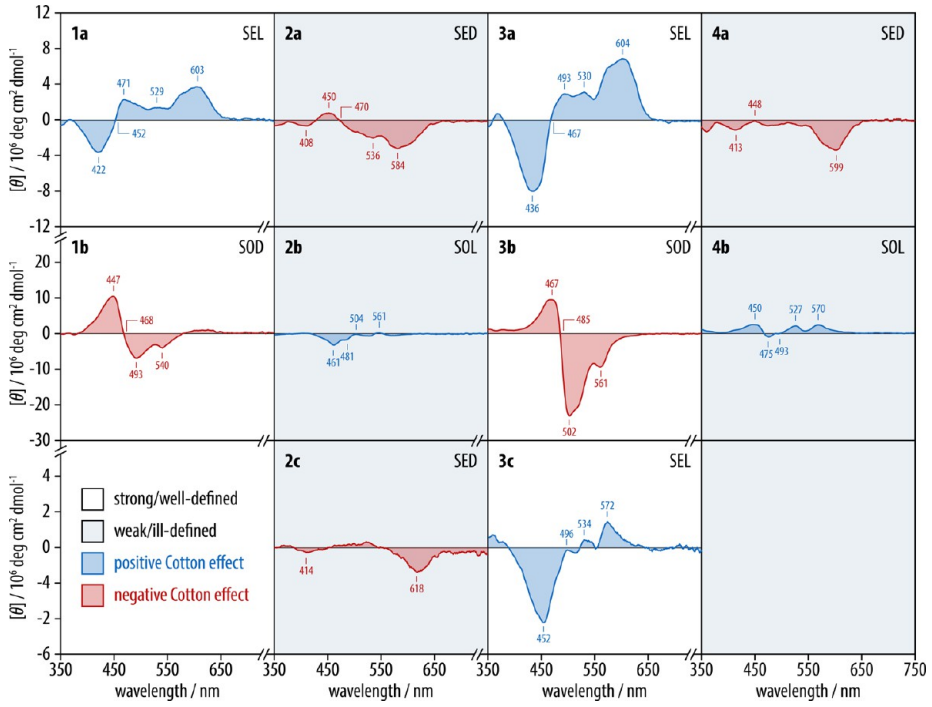

Figure 4. In solution-phase CD spectra (c = 1 × 10^{-4} mol/L, TCE, 293 K) of **1a**–**4a**, **1b**–**4b**, and **2c**, **3c** derivatives with an odd number of L-alanines per side group showed strong CD activity and well-defined CD spectra (white background, "anti-SED/SOL"), while CD spectra of derivatives with an even number of L-alanines were less resolved with undefined zero-crossings and much weaker signal intensities (gray backgrounds, "SED/SOL"). Furthermore, the CD spectra exhibited a two-fold odd–even effect in the sign of the Cotton effect (red = negative, blue = positive), alternatingly reversing with both the number of L-alanines and the length of the alkylene spacer.

not disturbed by a residual dipole moment, resulting in strong and well-defined CD spectra following the molecules' supposedly "anti-SED/SOL" preference. By contrast, the occurrence of "match/mismatch" pairs of the preferred handedness induced by the alkylene spacer and oligopeptide, respectively, can be excluded because it should result in a CD activity alternating in intensity with spacer length for oligo(L-alanine)s of a given length as well. Nevertheless, the self-assembly process is the result of the translation of molecular chirality into supramolecular helicity in competition with the molecules' inherent propensity to aggregate into β-sheet like superstructures. A simple oligopeptide β-strand composed of only L-amino acids is usually expected to attain a slightly right-handed twisted conformation that, upon aggregation, translates into a left-handed twisted β-sheet with a screw axis along the center of the β-sheet.[43] In the present case, however, two such β-sheet-like stacks are separated by the π–π-stacked chromophore, and the screw axis of the whole aggregate is placed along its center, which must inevitablely alter the oligopeptide aggregation pattern and imposes additional constraints such as those formulated in the SED/SOL rules.

Implications for Charge Transport. The well-defined and intense CD signals of some derivatives combined with the large energy splitting between hypsochromically and bathochromically shifted bands in the UV–vis spectra are an indication of a strong excitonic coupling. This can be regarded as a measure for constructive π-overlap between stacked perylene bisimides within the nanowires and, hence, as a proxy for percolation paths suitable for efficient charge transport. In order to test this hypothesis, we fabricated bottom-gate, bottom-contact field-effect transistors from monolayers of nanowires of **3a** and **4a**, obtained by spin coating of solutions onto prefabricated microchips with interdigitated source and drain gold electrodes (Figure 6). From the transfer curves of these field-effect tranistors in inert atmosphere, we preliminarily determined a lower estimate for the overall electron mobility of 8 × 10^{-7} cm^2 V^{-1} s^{-1} for the nanowire film of **3a** that was one order of magnitude higher than that of a comparable sample of a nanowire film of **4a** (9 × 10^{-8} cm^2 V^{-1} s^{-1}). These findings, hence, appear to correlate with the substantially different CD spectra of the two derivatives (see above), considering that both are equally strongly aggregated according to IR as well as UV–vis spectroscopy and give rise to well-defined nanofibrils.

CONCLUSIONS

We presented a detailed study on the structure–property relationship for a series of self-assembled nanowires from oligopeptide-polymer-substituted perylene bisimides comprising a varying number of L-alanines within the β-strands as well as differently long alkylene spacers between the central chromophore and the oligopeptide segments. Both UV–vis and CD spectroscopy showed that these suble differences in the molecular design significantly influenced the precise arrangement of the π–π-stacked chromophores within the aggregate. This was especially pronounced in the CD spectra, as they exhibited an unprecedented two-fold odd–even effect in regard to the intensity and sign of the Cotton effect as a function of the number of L-alanines and spacer length. The observation of both left- and right handed helical aggregates as well as assemblies with no global handedness is likely the result of a complex interplay between the "universal" translation of molecular chirality into supramolecular helicity and the molecules' inherent propensity for well-defined one-dimensional aggregation into β-sheet-like superstructures in the presence of a central chromophore. Thus, the observed formation of well-defined nanofibrils provides an illustrative

dx.doi.org/10.1021/ja412384p | J. Am. Chem. Soc. 2014, 136, 3919–3927

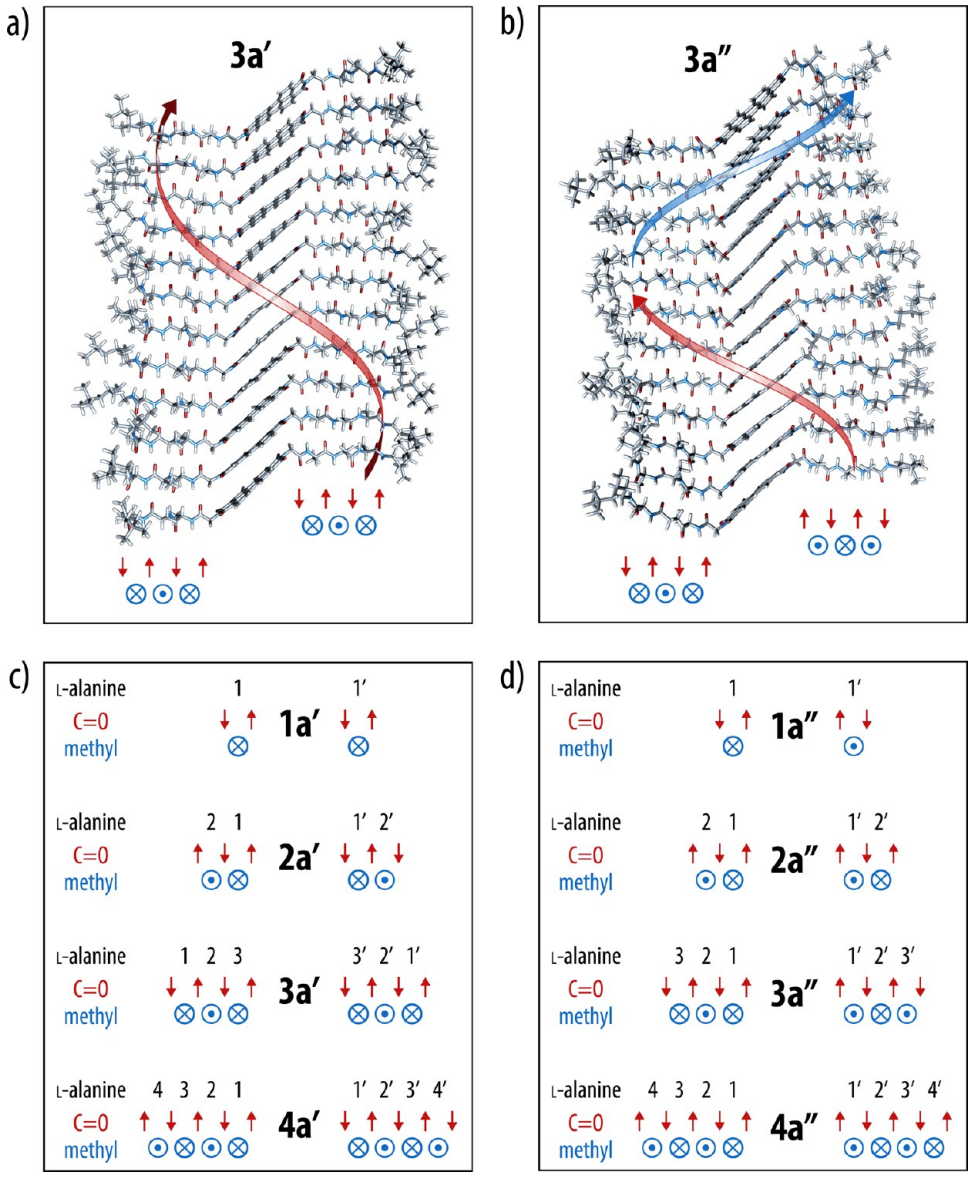

Figure 5. (a,b) MD simulations of the two stable suprameolecular arrangements of **3a** resulting from two different molecular conformations. The two innermost oligopeptide carbonyl groups (as indicated by the small arrows) in model **3a**′ were oriented in opposite directions, so as to minimize the global dipole moment of the assembly leading to a single-handed left-helical aggregate (curved red arrow). By contrast, they pointed into the same direction in model **3a**″, which results in a balanced steric load on the two faces of the β-sheet tapes (blue ⊗ and ⊙ indicate methyl groups pointing into and out of the plane of projection) but produces a formal nonzero residual dipole-moment for the derivatives with an even number of L-alanines. The resulting aggregate showed no global handedness but a transition from a left- (curved red arrow) to a right-handed helix (curved blue arrow). (c,d) Applying this formalism to all molecules within a series of a given spacer length revealed a formal odd−even effect that is depending on the overall steric and electronic interactions upon aggregation.

example for nanostructure and hierarchical structure formation by supramolecular self-assembly using as simple as possible sets of competing interactions.[44] This is particularly relevant in order to develop reliable design rules for self-assembled organic nanowires for several reasons. First of all, an unambiguous helicity of the supramolecular assembly renders the nanowires self-limiting with respect to lateral aggregation and bundle formation, which is the basis for obtaining well-defined nanowires. Second and more importantly, although a helical arrangement of the chromophores is not a prerequisite for efficient charge transport as such, our results demonstrate that even derivatives with similar molecular structures and self-assembly behavior can have significantly different charge transport properties that appear to correlate with the nature of their CD spectra. It is, hence, not generally sufficient to prepare one-dimensional aggregates of π-conjugated molecules in order to obtain self-assembled nanowires (as opposed to nonconducting nanofibrils). Instead, the exact molecular arrangement within the aggregates and, consequently, even supposedly minor details of the molecular structure may play an important role, which is a further reason to avoid overly complex molecular designs. In the case of oligopeptide-substituted chromophores such as those investigated here, all derivatives with more than $n = 2$ L-alanine residues per side group were strongly aggregated. But derivatives bearing an odd number of L-alanines in the side groups appear to be particularly promising candidates for further investigations of

dx.doi.org/10.1021/ja412384p | J. Am. Chem. Soc. 2014, 136, 3919−3927

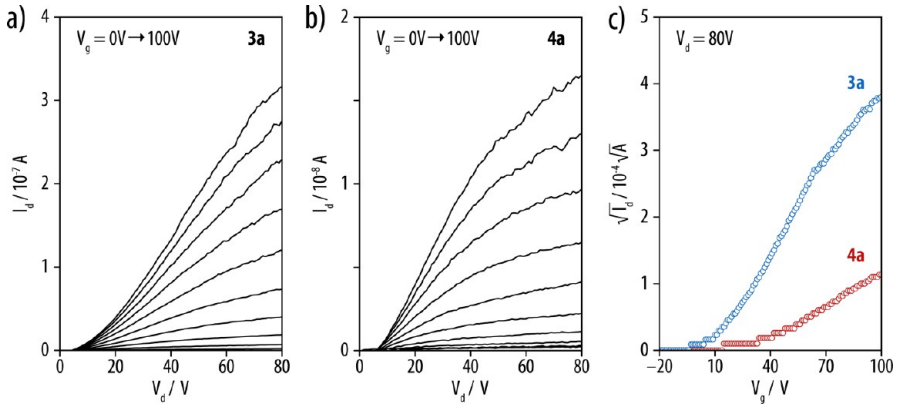

Figure 6. (a,b) Output- and (c) transfer curves obtained from measurements of field-effect transistors (in inert atmosphere) that had been fabricated by spin coating of nanowire solutions of **3a** and **4a** (c = 8.5 × 10^{-4} mol/L in TCE) onto generation 4 Fraunhofer n-doped silicon microchips with 230 nm SiO_2 gate dielectric and interdigitated gold source and drain contacts. The electron mobilities of 8 × 10^{-7} cm^2 V^{-1} s^{-1} for **3a** and 9 × 10^{-8} cm^2 V^{-1} s^{-1} for **4a** were derived from the maximum slopes of the transfer curves (measured at V_g = 80 V) and represent the lower estimate for a continuous thin film of the nanowires (including the electronically inactive parts of the film) with a channel length L = 2.5 μm and width W = 10 mm.

their electronic properties and macroscopic transport behavior in organic electronic devices.

■ ASSOCIATED CONTENT

Ⓢ Supporting Information

Figures S1−S2 and Schemes S1−S5 and details about IR, UV−vis, and CD spectroscopy as well as about AFM imaging. Details on the synthesis, NMR, and mass spectra of compounds **1a**−**4a**, **1b**−**4b**, **2c**, **3c**, **5**, and all intermediates as well as computational details. This material is available free of charge via the Internet at http://pubs.acs.org.

■ AUTHOR INFORMATION

Corresponding Author

holger.frauenrath@epfl.ch

Notes

The authors declare no competing financial interest.

■ ACKNOWLEDGMENTS

The authors would like to thank Prof. Clémence Corminboeuf (Ecole Polytechnique Fédérale de Lausanne, Switzerland) and Stephan N. Steinmann for providing the MD simulations. Furthermore, funding from the Swiss National Science Foundation (SNF Grants 200020_121812 and 200020_144417) is gratefully acknowledged.

■ REFERENCES

(1) Hoeben, F. J. M.; Jonkheijm, P.; Meijer, E. W.; Schenning, A. P. H. J. *Chem. Rev.* **2005**, *105*, 1491.

(2) Schenning, A. P. H. J.; Meijer, E. W. *Chem. Commun.* **2005**, 3245.

(3) Xiao, S.; Tang, J.; Beetz, T.; Guo, X.; Tremblay, N.; Siegrist, T.; Zhu, Y.; Steigerwald, M.; Nuckolls, C. *J. Am. Chem. Soc.* **2006**, *128*, 10700.

(4) Jonkheijm, P.; Stutzmann, N.; Chen, Z.; de Leeuw, D. M.; Meijer, E. W.; Schenning, A. P. H. J.; Würthner, F. *J. Am. Chem. Soc.* **2006**, *128*, 9535.

(5) Briseno, A. L.; Mannsfeld, S. C. B.; Lu, X.; Xiong, Y.; Jenekhe, S. A.; Bao, Z.; Xia, Y. *Nano Lett.* **2007**, *7*, 668.

(6) Briseno, A. L.; Mannsfeld, S. C. B.; Jenekhe, S. A.; Bao, Z.; Xia, Y. *Mater. Today* **2008**, *11*, 38.

(7) Finlayson, C. E.; Friend, R. H.; Otten, M. B. J.; Schwartz, E.; Cornelissen, J. J. L. M.; Nolte, R. J. M.; Rowan, A. E.; Samorì, P.; Palermo, V.; Liscio, A.; Peneva, K.; Müllen, K.; Trapani, S.; Beljonne, D. *Adv. Funct. Mater.* **2008**, *18*, 3947.

(8) Yamamoto, Y.; Zhang, G.; Jin, W.; Fukushima, T.; Ishii, N.; Saeki, A.; Seki, S.; Tagawa, S.; Minari, T.; Tsukagoshi, K.; Aida, T. *Proc. Natl. Acad. Sci. U.S.A.* **2009**, *106*, 21051.

(9) Garcia-Frutos, E. M. *J. Mater. Chem. C* **2013**, *1*, 3633.

(10) Schmidt-Mende, L.; Fechtenkötter, A.; Müllen, K.; Moons, E.; Friend, R. H.; MacKenzie, J. D. *Science* **2001**, *293*, 1119.

(11) Palermo, V.; Otten, M. B. J.; Liscio, A.; Schwartz, E.; de Witte, P. A. J.; Castriciano, M. A.; Wienk, M. M.; Nolde, F.; De Luca, G.; Cornelissen, J. J. L. M.; Janssen, R. A. J.; Müllen, K.; Rowan, A. E.; Nolte, R. J. M.; Samorì, P. *J. Am. Chem. Soc.* **2008**, *130*, 14605.

(12) Xin, H.; Kim, F. S.; Jenekhe, S. A. *J. Am. Chem. Soc.* **2008**, *130*, 5424.

(13) Wicklein, A.; Ghosh, S.; Sommer, M.; Würthner, F.; Thelakkat, M. *ACS Nano* **2009**, *3*, 1107.

(14) Chen, J.-T.; Hsu, C.-S. *Polym. Chem.* **2011**, *2*, 2707.

(15) Katz, H. E. *Electroanal.* **2004**, *16*, 1837.

(16) Zang, L.; Che, Y.; Moore, J. S. *Acc. Chem. Res.* **2008**, *41*, 1596.

(17) Che, Y.; Yang, X.; Loser, S.; Zang, L. *Nano Lett.* **2008**, *8*, 2219.

(18) Zhao, Y. S.; Wu, J.; Huang, J. *J. Am. Chem. Soc.* **2009**, *131*, 3158.

(19) Che, Y.; Gross, D. E.; Huang, H.; Yang, D.; Yang, X.; Discekici, E.; Xue, Z.; Zhao, H.; Moore, J. S.; Zang, L. *J. Am. Chem. Soc.* **2012**, *134*, 4978.

(20) Hernando, J.; de Witte, P. A. J.; van Dijk, E. M. H. P.; Korterik, J.; Nolte, R. J. M.; Rowan, A. E.; García-Parajó, M. F.; van Hulst, N. F. *Angew. Chem., Int. Ed.* **2004**, *43*, 4045.

(21) Würthner, F.; Bauer, C.; Stepanenko, V.; Yagai, S. *Adv. Mater.* **2008**, *20*, 1695.

(22) Lee, C. C.; Grenier, C.; Meijer, E. W.; Schenning, A. P. H. J. *Chem. Soc. Rev.* **2009**, *38*, 671.

(23) Vadehra, G. S.; Wall, B. D.; Diegelmann, S. R.; Tovar, J. D. *Chem. Commun.* **2010**, *46*, 3947.

(24) Gray, G. W.; McDonnell, D. G. *Mol. Cryst. Liq. Cryst.* **1976**, *34*, 211.

(25) Goodby, J. W.; Leslie, T. M. *Mol. Cryst. Liq. Cryst.* **1984**, *110*, 175.

(26) Goodby, J. W.; Chin, E.; Leslie, T. M.; Geary, J. M.; Patel, J. S. *J. Am. Chem. Soc.* **1986**, *108*, 4729.

(27) Ramos Lermo, E.; M. W. Langeveld-Voss, B.; A. J. Janssen, R.; W. Meijer, E. *Chem. Commun.* **1999**, 791.

(28) Amabilino, D. B.; Serrano, J.-L.; Sierra, T.; Veciana, J. *J. Polym. Sci., Part A: Polym. Chem.* **2006**, *44*, 3161.

(29) Zhi, J.; Zhu, Z.; Liu, A.; Cui, J.; Wan, X.; Zhou, Q. *Macromolecules* **2008**, *41*, 1594.

(30) Henze, O.; Feast, W. J.; Gardebien, F.; Jonkheijm, P.; Lazzaroni, R.; Leclère, P.; Meijer, E. W.; Schenning, A. P. H. J. *J. Am. Chem. Soc.* **2006**, *128*, 5923.
(31) Marty, R.; Szilluweit, R.; Sánchez-Ferrer, A.; Bolisetty, S.; Adamcik, J.; Mezzenga, R.; Spitzner, E.-C.; Feifer, M.; Steinmann, S. N.; Corminboeuf, C.; Frauenrath, H. *ACS Nano* **2013**, *7*, 8498.
(32) Würthner, F.; Sautter, A.; Schmid, D.; Weber, P. J. A. *Chem.—Eur. J.* **2001**, *7*, 894.
(33) Tian, L. F.; Szilluweit, R.; Marty, R.; Bertschi, L.; Zerson, M.; Spitzner, E. C.; Magerle, R.; Frauenrath, H. *Chem. Sci.* **2012**, *3*, 1512.
(34) Akers, K.; Aroca, R.; Hor, A. M.; Loufty, R. O. *Spectrochim. Acta* **1988**, *44A*, 1129.
(35) Stepanenko, V.; Li, X.-Q.; Gershberg, J.; Würthner, F. *Chem.—Eur. J.* **2013**, *19*, 4176.
(36) Molla, M. R.; Ghosh, S. *Chem. Mater.* **2010**, *23*, 95.
(37) Chen, Z.; Stepanenko, V.; Dehm, V.; Prins, P.; Siebbeles, L. D. A.; Seibt, J.; Marquetand, P.; Engel, V.; Würthner, F. *Chem.—Eur. J.* **2007**, *13*, 436.
(38) Thalacker, C.; Würthner, F. *Adv. Funct. Mater.* **2002**, *12*, 209.
(39) Dehm, V.; Chen, Z.; Baumeister, U.; Prins, P.; Siebbeles, L. D. A.; Würthner, F. *Org. Lett.* **2007**, *9*, 1085.
(40) Henze, O.; Feast, W. J.; Gardebien, F.; Jonkheijm, P.; Lazzaroni, R.; Leclere, P.; Meijer, E. W.; Schenning, A. P. H. J. *J. Am. Chem. Soc.* **2006**, *128*, 5923.
(41) Stals, P. J. M.; Smulders, M. M. J.; Martín-Rapún, R.; Palmans, A. R. A.; Meijer, E. W. *Chem.—Eur. J.* **2009**, *15*, 2071.
(42) Nakano, Y.; Hirose, T.; Stals, P. J. M.; Meijer, E. W.; Palmans, A. R. A. *Chem. Sci.* **2012**, *3*, 148.
(43) Aggeli, A.; Nyrkova, I. A.; Bell, M.; Harding, R.; Carrick, L.; McLeish, T. C. B.; Semenov, A. N.; Boden, N. *Proc. Natl. Acad. Sci. U.S.A.* **2001**, *98*, 11857.
(44) Muthukumar, M.; Ober, C. K.; Thomas, E. L. *Science* **1997**, *277*, 1225.